



This is a repository copy of *Process modelling, validation and analysis of rotating packed bed stripper in the context of intensified CO₂ capture with MEA.*

White Rose Research Online URL for this paper:

<https://eprints.whiterose.ac.uk/146675/>

Version: Accepted Version

Article:

Borhani, T.N., Oko, E. orcid.org/0000-0001-9221-680X and Wang, M. orcid.org/0000-0001-9752-270X (2019) Process modelling, validation and analysis of rotating packed bed stripper in the context of intensified CO₂ capture with MEA. *Journal of Industrial and Engineering Chemistry*, 75. pp. 285-295. ISSN 1226-086X

<https://doi.org/10.1016/j.jiec.2019.03.040>

Article available under the terms of the CC-BY-NC-ND licence (<https://creativecommons.org/licenses/by-nc-nd/4.0/>).

Reuse

This article is distributed under the terms of the Creative Commons Attribution-NonCommercial-NoDerivs (CC BY-NC-ND) licence. This licence only allows you to download this work and share it with others as long as you credit the authors, but you can't change the article in any way or use it commercially. More information and the full terms of the licence here: <https://creativecommons.org/licenses/>

Takedown

If you consider content in White Rose Research Online to be in breach of UK law, please notify us by emailing eprints@whiterose.ac.uk including the URL of the record and the reason for the withdrawal request.



eprints@whiterose.ac.uk
<https://eprints.whiterose.ac.uk/>

Process modelling, validation and analysis of rotating packed bed stripper in the context of intensified CO₂ capture with MEA

Tohid N.Borhani^a, Eni Oko^a and Meihong Wang^{*a}

^aDepartment of Chemical and Biological Engineering, The University of Sheffield, Sheffield S1 3JD, UK

Abstract

Rotating packed bed (RPB) system has applications in CO₂ removal using chemical solvents which can reduce the size about ten times compared to common packed bed (PB) system. In this study, RPB stripper using monoethanolamine (MEA) solution is modelled in gPROMS[®] software. The model has been validated using experimental data from literature and show good agreement. In addition to stripper modelling and validation, the process analysis is accomplished in this study by assessing the influence of four parameters namely rotor speed, reboiler temperature, flow rate of rich liquid, and pressure on desorption efficiency and desorption energy.

Keywords: Carbon capture, process intensification, rotating packed bed, stripper, monoethanolamine, process analysis.

Nomenclature

a_{gl}	Gas – liquid interfacial area (m ² /m ³)
C_i	Molar concentration of component i in liquid phase (kmol/m ³)
E_i	The enhancement factor of component i
F	The flow rate of the liquid stream leaving the stripper (kmol/s)
F_g	The molar flow rate of the gas phase in RPB (kmol/s)
F_l	The molar flow rate of the liquid phase in RPB (kmol/s)
H_F	Liquid enthalpy entering the reboiler (kJ/mol)
H_L	Liquid enthalpy leaving the reboiler (kJ/mol)
H_V	Vapor enthalpy leaving the reboiler (kJ/mol)
h_{gl}	Heat transfer coefficient (W/(m ² . K))
$He_{l,i}$	Henry's constant of component i in liquid solution (kPa. m ³ /kmol)
h_{out}	The wall heat transfer coefficient of stripper
$k_{g,i}$	Mass transfer coefficient of component i in the gas phase (m/s)
$K_{g,i}$	Overall mass transfer coefficient of gas for component i (kmol/(m ² . kPa. s))
K_{eq}	Equilibrium reaction constants

* Corresponding author.

E-mail address: meihong.wang@sheffield.ac.uk (Professor Meihong Wang)

Tel.: +44(0)1142227160

$k_{l,i}$	The mass transfer coefficient of component i in the liquid phase (m/s)
k_{obs}	Observed reaction rate constant based (1/s)
$K\text{-value}_i$	Vapor-liquid equilibrium ratio
L	The flow rate of liquid stream leaving the reboiler (lean MEA liquid stream) (kmol/s)
N_i	Molar flux of component i (kmol/(m ² .s))
P_i	The partial pressure of component i in the bulk gas (kPa)
P_i^*	Equilibrium partial pressure of component i corresponding to its concentration in the bulk liquid (kPa)
P_{motor}	The motor power (kW)
Q_l	Volumetric flow rate of liquid phase (l/min)
Q_{reb}	Heat duty of reboiler (kW)
q_g	Heat transfer flux in gas phase (W/m ²)
q_l	Heat transfer flux in liquid phase (W/m ²)
q_l^{loss}	Heat loss from liquid phase to ambient
R_i	The inner radius of RPB (m)
R_o	The outer radius of RPB (m)
R_g	Universal gas constant (kPa. m ³ /(kmol. K))
T_{amb}	The ambient temperature (K)
T_g	Gas phase temperature (K)
$T_{g,0}$	Gas phase temperature in the inlet (K)
T_l	Liquid phase temperature (K)
$T_{l,0}$	Liquid phase temperature in the inlet (K)
V	The flow rate of vapour stream leaving the reboiler (kmol/s)
x_i	The mole fraction of component i in the liquid phase
x_0	The mole fraction of component i in the inlet liquid phase (initial mole fraction)
y_i	The mole fraction of component i in the gas phase
y_0	The mole fraction of component i in the inlet gas phase (initial mole fraction)
z_i	The mole fraction of component i in the inlet to reboiler
Z	The axial height of the packing (m)

Greek Symbols

α_{CO_2}	CO ₂ loading (mol CO ₂ /mol MEA)
ε	The porosity of packing (m ³ /m ³)
ε_L	Liquid hold-up
ΔH_{Des}	The heat of desorption of CO ₂ (J/kmol)
ΔH_{vap}	The heat of vaporization of H ₂ O (J/kmol)

Abbreviations

AARD	Average absolute relative deviation
ARD	Average relative deviation
CFDM	Centred finite difference method
GA	Genetic algorithm
GJ	Gigajoule
MLR	Multiple linear regression
PB	Packed bed
RPB	Rotating packed bed
VLE	Vapor liquid equilibrium

1 Introduction

1.1 Background

Global warming is a very serious problem and anthropogenic CO₂ emission is one of the biggest contributors to this phenomena [1]. Most of the CO₂ are emitted from different industries. For instances, coal combustion in a 500 MWe coal-fired power plant produces 8000-10000 tons of CO₂ per day while a similar capacity natural gas combined cycle power plant produces about 4000 tons of CO₂ per day. Through carbon capture and storage (CCS), the CO₂ emitted from these sources can be prevented from entering the atmosphere. CO₂ separation in carbon capture process can be achieved through different technologies: absorption, adsorption, membrane, and cryogenic among others. Among these technologies, absorption in which a liquid solution (solvent) is used to capture CO₂ from the gas stream is the most matured and commercially-ready option. Different solvents categorized as chemical, physical and chemical-physical are applied in absorption processes [2]. Among these solvents, amines which are chemical solvents with monoethanolamine (MEA) as a typical example are the commonest options for gas stream applications with low CO₂ partial pressure *e.g.* power plant flue gases. MEA is well researched in literature and is considered to be the benchmark solvent in this process.

The CO₂ absorption process contains different unit operations which one of the most important and key units is the stripper. This unit, which is also well-known as regenerator or desorber, regenerates the solvent by using the maximum energy that is required in the CO₂ capture system. It should be noted that about 60% of the required energy in CO₂ capture process using absorption is utilized to regenerate the solvent and this high energy consumption has been considered a big obstacle for solvent-based technology [3]. Three important strategies have been used to decrease the energy requirement of stripper (a) development of new solvents or improvement of existing solvents by adding other solvents (solvent mixtures) [4]; (b) improvement of the process (*e.g.* by increasing mass and heat transfer by using RPB) [5], membrane [6] or changing the process configuration [7]); (c) optimization of operating parameters of the process (*e.g.* CO₂ loading and solvent concentration) [8].

In order to assess the impact of different operating conditions on the process configuration and solvent type, the stripper model development is necessary. A validated and trustable stripper model can be used

for optimization, scale up, process analysis, configuration analysis and finding the best operating parameters. The insight from the assessment also will be useful for solvent development, process design and development. This will also improve the understanding of the stripper operation and inspire energy-saving designs to reduce the energy penalty of the process. Finally, it will support commercial-scale stripper design and development [9]. In the stripper, CO₂ strips from the solvent and the solvent can be recycled to the absorber. When the partial pressure of CO₂ in the gas phase is smaller than the equilibrium partial pressure of CO₂ in the rich solution, the desorption phenomena happens. When MEA is the solvent, the typical reboiler temperature changes from 110 to 120 °C and it is recommended avoid liquid temperatures more than 120 °C in the stripper column due to solvent degradation issue [10]. The required heat for the stripper (desorption heat duty) is provided by steam in the reboiler and can be estimated as the contribution of three terms:

- (i) *The heat of desorption* to reverse the chemical reactions between the solvent and CO₂ (heat of reaction) and breaking the chemical bonds between CO₂ and solvent and drive out the CO₂ from the liquid (heat of dissolution).
- (ii) *Latent heat of vaporization* to produce steam to decrease the solubility of the CO₂ in the solution and the partial pressure of CO₂ in the gas phase.
- (iii) *Sensible heat* to heat up the rich amine solution for the solvent desorption in the stripper column.

Oxemann and Kather [11] described the importance of accounting all three contributors in the overall desorption heat duty. They reported that in many solvent screening studies the authors considered only one contributor (heat of desorption) to select the solvent and neglected the two other contributors. This assumption will result in a misleading conclusion. The temperature of reboiler will also determine the CO₂ loading in the lean MEA liquid stream that will affect the CO₂ absorption in the absorber column. Therefore, the temperature of reboiler is a key operational constraint that must be controlled properly [10].

Despite the importance of stripper in the CO₂ capture process, there are a few numbers of experimental studies available in the literature. The performance of MEA and DEA solutions is compared experimentally by considering different stripping conditions in a lab pilot plant packed bed [12]. The

authors investigated the relationship between regeneration energy and operation conditions of the stripper. They suggested two methods to decrease the heat duty of reboiler the first one is the application of proper solvent flow rate and also proper lean loading and the second one is the application of higher concentrations of solvents up to a certain level. They also reported that the performance of rich/lean heat exchanger has a great effect on the reboiler heat duty. In another experimental study, the energy requirement for CO₂ capture using MEA and MEA-MDEA solutions was examined [13]. They examined the effect of different parameters on the energy consumption of the packed bed system.

In addition to experimental studies, different stripper model studies are presented for packed beds (PBs) [14, 15]. According to literature, modelling of the stripper is more complex in comparison with the absorber. In addition to the stripper column model, the model of reboiler and in some cases the condenser are required as well. One of the first stripper modelling studies is presented by Weiland et al. [16]. The authors mentioned that for stripper the chemical reactions should be considered as reversible reactions and hence chemical thermodynamics come in the stripping calculations [16]. The authors also mentioned that in desorption, the mass transfer resistances in both gas and liquid phases have equal importance. This is unlike the absorption process which liquid phase resistance, is predominant mainly. Mores et al. [15] optimized the operating conditions (pressures, temperatures and flow-rates) and dimensions (diameter and height) of the MEA desorption unit using nonlinear programming (NLP) mathematical model in GAMS. The authors used the equilibrium stage approach by using Murphree efficiency. Khalilpour and Abbas [17] explained in detail that the most critical and important parameters in stripper are reboiler pressure and temperature and gas stream flow rate in the column. They described different constraint required for design and modelling of the stripper. Li and Keener [18] reviewed different studies on stripper using a different type of solvents. The authors compared and discussed the implementation of different solvents, the recently established methods, the addition of acids, membrane equipment, and dual alkali method with the usual heating process. In addition to mentioned stripper modelling studies, there are some studies that focused on the process configuration for stripper [7, 19].

The energy consumption in the stripper can be reduced through process improvement. Process intensification (PI) is a typical technology for process improvement and has been applied successfully

in different areas. Among all the PI technologies studied, rotating packed bed (RPB) proves to be the most suitable for intensified carbon capture process due to its scalability and some researchers have successfully used RPB instead of PB for CO₂ capture applications [20]. It has also been used in other gas-liquid processes such as H₂S absorption [21], liquid-liquid processes such as liquid liquid extraction [22] and also in solid-liquid processes such as adsorption. As mentioned in the previous study [23], utilizing RPBs can increase the mass transfer rate significantly which leads to substantial size and weight reduction of the equipment. In addition, RPBs can reduce the energy consumption due to lower solvent inventory compared to PBs. In RPBs, stronger solvent concentration are mainly used and this contributes to lower solvent circulation rate. In MEA case, the stronger solution has lower heat capacity and water fraction which contributes to overall lower sensible heat duty [24].

The RPBs also showed a wider flooding limit. The wider flooding limit is mainly due to centrifugal forces, which allows for higher L/G ratio without flooding. This is also the main reason for the reduced size of the RPB-stripper. Furthermore, the RPBs are appropriate for short contact time instances because of the reduced packing volume of the RPBs. It was also reported that the RPB has better self-cleaning and avoidance of blocking in comparison with PBs. Similar to PB, RPB can be utilized as both absorber and stripper [20]. The total cost of the RPB-based process is expected to be lower. Joel [25] showed that the total cost of RPB-based solvent CO₂ capture for capture from an NGCC power plant is about €61/tCO₂ compared to about €65/tCO₂ for the PB-based technology.

1.2 Review of previous studies on RPB stripper modelling

Even for PBs, the number of studies performed for the modelling of the stripper is considerably less than the number of studies done for the absorber. In the case of RPB stripper, there is only one study which is performed by Joel et al. [26]. The authors utilized ASPEN PLUS[®] in combination with FORTRAN[®]. They used visual FORTRAN[®] as subroutines and inserted the mass transfer coefficients equations for liquid and gas phases, heat transfer coefficient, and hydrodynamic parameters appropriate for RPB system. They dynamically linked FORTRAN[®] with ASPEN PLUS[®]. They used two sets of experimental data to validate their model. The data presented by Jassim et al. [27] and data of Cheng et al. [5] are used to validate their model. After the validation of the model, they performed process

analysis. Furthermore, the authors compared the RPB and PB stripper models under the same process conditions and reported a volume reduction of 9.691. Therefore, the current study is the first process modelling of RPB stripper using equation-oriented approach. In this approach, all the governing equations of the system are considered by the researcher and the related models to predict physical properties can be selected according to the system. Therefore, using the approach help the researcher to understand the effect of different parameters clearly and change them easily to achieve the appropriate results [28].

1.3 Novel contributions of the study

This is the first equation-oriented distributed steady state rate-based model on RPB stripper system developed in gPROMS[®]. Four novelty of this study are: (a) a steady state first principle rate-based model for RPB stripper via equation-oriented approach was developed and fulfilled in gPROMS[®]. The model is validated using the data from literature [5, 27]; (b) experimental data of partial pressure of CO₂ from literature are correlated using regression method and the correlation utilized to calculate the partial pressure of CO₂ and heat of desorption in the RPB stripper; (c) the K-value required in reboiler calculations is constructed using data from Aspen Plus and using GA-MLR method; (d) the process analysis done to realize the influence of different operating parameters on the modelling results and the results are compared with the process analysis reported by Cheng et al. [5] and also Joel et al. [26]. Different and inclusive conditions of changing rotor speed, reboiler temperature, rich liquid flow rate, and pressure are considered in these analyses.

2 Model development

In order to develop the steady-state RPB stripper model, some assumptions have been considered as follow:

- The gas phase is ideal and contains CO₂, H₂O, and N₂
- The liquid phase consists of CO₂, H₂O, MEA, and ionic species namely HCO₃⁻, CO₃²⁻, OH⁻, H₃O⁺, MEAH⁺, and MEACOO⁻
- The model accounted only mass transfer flux of CO₂, H₂O, N₂, and MEA

- Fluid flows in radial direction
- There is no any end effect in the RPB stripper and all the reactions happen in the liquid film
- The phases contact to each other counter currently
- The specified rich loading is achievable from the absorber (the absorber was not modelled in this study)
- The reboiler is in vapor-liquid equilibrium

In continue of this section the main elements of RPB stripper model are presented in great detail. It should be noted that, due to the high-temperature difference between stripper and ambient, heat losses are also taken into account.

2.1 Equations for stripper

In the RPB the radial direction is considered as the direction of concentration change for the components. The mass and heat balances (the governing equations) for both phases can be written as follow [24]:

$$\frac{\partial(F_g y_i)}{\partial r} = a_{gl} N_i (2\pi r z) \quad \text{B. C.:} \begin{cases} \text{at } r = R_o : y_i = y_0 \\ \text{at } r = R_i : \frac{\partial(F_g y_i)}{\partial r} = 0 \end{cases} \quad (1)$$

$$\frac{\partial(F_l x_i)}{\partial r} = a_{gl} N_i (2\pi r z) \quad \text{B. C.:} \begin{cases} \text{at } r = R_i : x_i = x_0 \\ \text{at } r = R_o : \frac{\partial(F_l x_i)}{\partial r} = 0 \end{cases} \quad (2)$$

$$\frac{\partial(F_g C_{pg} T_g)}{\partial r} = a_{gl} q_g (2\pi r z) \quad \text{B. C.:} \begin{cases} \text{at } r = R_o : T_g = T_{g,0} \\ \text{at } r = R_i : \frac{\partial(F_g C_{pg} T_g)}{\partial r} = 0 \end{cases} \quad (3)$$

$$\frac{\partial(F_l C_{pl} T_l)}{\partial r} = a_{gl} q_l (2\pi r z) \quad \text{B. C.:} \begin{cases} \text{at } r = R_i : T_l = T_{l,0} \\ \text{at } r = R_o : \frac{\partial(F_l C_{pl} T_l)}{\partial r} = 0 \end{cases} \quad (4)$$

2.2 Equations for reboiler

The most important part of a stripper unit is reboiler that provides the required heat for desorption. The reboiler model in this study represented as a single equilibrium steady-state stage. The reboiler equations are flash calculation as follow [29]:

$$F = L + V \quad (5)$$

$$z_i F = x_i L + y_i V \quad (6)$$

$$\sum x_i = 1, \sum y_i = 1 \quad (7)$$

$$K\text{-value}_i = \frac{y_i}{x_i} \quad (8)$$

$$FH_F + Q_{reb} = LH_L + VH_V \quad (9)$$

F is the flow rate of the liquid stream leaving the stripper and is the inlet to the reboiler. L is the flow rate of the liquid stream leaving the reboiler (lean MEA liquid stream). V is the flow rate of the vapor stream leaving the reboiler and is the inlet to the bottom of the stripper. H_F and H_L are liquid enthalpies entering and leaving the reboiler. H_V is the vapor enthalpy leaving the reboiler and Q_{reb} is the heat duty of reboiler. K-values are values to calculate the VLE which is required for reboiler. The K-values data are collected from Aspen Plus® by considering a range of mole fraction and temperatures. In order to find the best parameters effective on the K-values, the genetic algorithm in combination with multiple linear regression (GA-MLR) is used to develop a regression model for K-values in Matlab (see section 2.6).

2.3 Mass and heat rate equations

The two-film theory has wide applications in modelling CO₂ absorption and desorption in different types of absorbers and strippers when describing the mass transfer between two liquid and gas phases. This theory offers simpler mathematical equations and also a considerable number of mass transfer coefficient correlations were developed based on this theory. In the current study, the following mass transfer flux is considered [30]:

$$N_i = K_{g,i}(P_i - P_i^*) \quad (10)$$

where P_i and P_i^* (kPa) are the partial pressure of component i in the gas phase and the equilibrium partial pressure of component i in the bulk liquid, respectively. $K_{g,i}$ is the overall mass transfer coefficients of component i based on the gas phase that is estimated by the subsequent equation [30]:

$$\frac{1}{K_{g,i}} = \frac{R_g T_g}{k_{g,i}} + \frac{H_{e1,i}}{E_i k_{l,i}} \quad (11)$$

where $k_{g,i}$ and $k_{l,i}$ are the gas and liquid side mass transfer coefficient of component i , respectively. The effect of chemical reaction in the system on the mass transfer is considered utilizing the enhancement factor (E_i). $He_{l,i}$ is Henry's constant for insoluble gases in the liquid phase. In the liquid phase for solvents namely water and monoethanolamine, the resistance to mass transfer is insignificant. Therefore, the following mass transfer rate equations are used in the modelling of RPB stripper [30]:

$$N_{\text{MEA}} = \frac{k_{g,\text{MEA}}}{R_g T_g} (P_{\text{MEA}} - P_{\text{MEA}}^*) \quad (12)$$

$$N_{\text{H}_2\text{O}} = \frac{k_{g,\text{H}_2\text{O}}}{R_g T_g} (P_{\text{H}_2\text{O}} - P_{\text{H}_2\text{O}}^*) \quad (13)$$

$$N_{\text{CO}_2} = \frac{1}{\frac{R_g T_g}{k_{g,\text{CO}_2}} + \frac{He_{l,\text{CO}_2}}{E_{\text{CO}_2} k_{l,\text{CO}_2}}} (P_{\text{CO}_2} - P_{\text{CO}_2}^*) \quad (14)$$

In Eq. (12)-(14), the multiplication of mole fraction in the gas phase and the total pressure of gas phase (P) result in P_i values and the VLE calculations (Section 2.5) provide P_i^* values. The heat transfer rate can be written as [31]:

$$q_g = h_{gl}(T_l - T_g) \quad (15)$$

$$q_l = h_{gl}(T_l - T_g) + \Delta H_{\text{Des}} N_{\text{CO}_2} + \Delta H_{\text{vap}} N_{\text{H}_2\text{O}} + q_l^{\text{loss}} \quad (16)$$

where h_{gl} is the heat transfer coefficient, T_l and T_g are the temperature of the liquid and gas phase, respectively. ΔH_{Des} is the heat of desorption of CO_2 , ΔH_{vap} is the heat of vaporization of H_2O . The heat loss in the stripper is calculate based on the temperature difference between liquid temperature and ambient temperature [10]:

$$q_l^{\text{loss}} = h_{\text{out}}(T_l - T_{\text{amb}}) \quad (17)$$

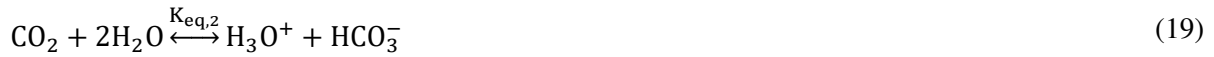
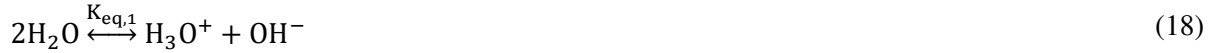
where h_{out} is the heat transfer coefficient of the wall of stripper and T_{amb} is the ambient temperature.

2.4 Effects of chemical reactions on the model

When the rate-based modelling approach is considered, the influence of chemical reactions should be accounted for in the main governing equations of the system.

2.4.1 Chemical reactions

When CO₂ absorbs in the MEA aqueous solution, the following reactions may occur. These reactions are considered by different researchers as dominated reactions [32]:



where K_{eq} is equilibrium constants. It was assumed that these reactions reached equilibrium. In this study, reactions (18) to (22) are utilized in VLE and speciation calculation (section 2.5). In addition to above-mentioned reactions, the following overall reaction can also be considered [33]:



Reaction (23) is interpreted using two important mechanisms namely zwitterion and termolecular in the literature. Based on these two well-known mechanisms, two different types of kinetic model can be considered for the reaction between CO₂ and MEA. The details about these kinetic models that have an important effect on the result of the model are presented in Borhani et al. [23].

2.4.2 Enhancement factor

In order to account the chemical reactions in the rate-based stripper model, there are two main ways. The first is the consideration of mass transfer with equilibrium reaction which this approach used by many researchers. In this method, it is assumed that the mass transfer in the stripper is accompanied by an equilibrium reversible (instantaneous) reaction. Consequently, there is a chemical equilibrium throughout the liquid phase [34]. On the other hand, the second method is the combination of mass transfer and the reaction kinetic in the liquid boundary layer. It must be mentioned that the second method is used by a few researchers [14]. Enhancement factor is a parameter to include the chemical reaction into the mass transfer rate equations. Therefore, based on the two above mentioned ways of accounting chemical reactions, two types of enhancement factors can be used in the stripper modeling.

Tobiesen et al. [35] explained that the reaction kinetics of desorption is different from the absorption due to the high temperature of the desorption process. Astarita and Savage [34] gave details about desorption by having equilibrium reversible reactions and presented a comprehensive analytical solution for the film model and numerical solution of penetration model. Therefore, in the stripper, Tobiesen et al. [35] assumed that there is mass transfer with a reversible instantaneous reaction at equilibrium for CO₂ and MEA.

However, Oyenekan and Rochelle [14] and Mores et al. [15] utilized the kinetic reaction to calculate the enhancement factor for stripper modelling. In this study, the second approach has been used. As it was shown in our previous study the following relation is utilized to evaluate the enhancement factor:

$$E_{\text{Stripper}} = \frac{\sqrt{k_{\text{obs}} D_{1,\text{CO}_2}}}{k_{1,\text{CO}_2}} \quad (24)$$

where k_{obs} is the observed reaction rate constant which is calculated based on reaction (23). D_{1,CO_2} is diffusivity of CO₂ in the lean MEA solution and k_{1,CO_2} is the mass transfer coefficient of CO₂ in lean MEA solution. In this study, the k_{obs} defined in the previous study [23] have been used.

2.5 Equilibrium calculations

These calculations include vapour-liquid equilibrium (VLE) calculations and speciation equilibrium calculations (chemical equilibrium calculations).

2.5.1 Chemical equilibrium

In this study, the following equations are utilized to calculate the chemical equilibrium which is well-known as speciation calculation. The constants value in the right side of the equations are extracted from [36] and [37]:

$$K_{\text{eq},1} = \gamma_{\text{OH}^-} \cdot \gamma_{\text{H}_3\text{O}^+} \cdot C_{\text{OH}^-} \cdot C_{\text{H}_3\text{O}^+} = \exp\left(140.932 - \frac{13445.9}{T_1} - 22.4773 \ln T_1\right) \quad (25)$$

$$K_{\text{eq},2} = \frac{\gamma_{\text{HCO}_3^-} \cdot \gamma_{\text{H}_3\text{O}^+}}{\gamma_{\text{CO}_2}} \cdot \frac{C_{\text{HCO}_3^-} \cdot C_{\text{H}_3\text{O}^+}}{C_{\text{CO}_2}} = \exp\left(235.482 - \frac{12092.1}{T_1} - 36.7816 \ln T_1\right) \quad (26)$$

$$K_{\text{eq},3} = \frac{\gamma_{\text{CO}_3^{2-}} \cdot \gamma_{\text{H}_3\text{O}^+}}{\gamma_{\text{HCO}_3^-}} \cdot \frac{C_{\text{CO}_3^{2-}} \cdot C_{\text{H}_3\text{O}^+}}{C_{\text{HCO}_3^-}} = \exp\left(220.067 - \frac{12431.7}{T_1} - 35.4819 \ln T_1\right) \quad (27)$$

$$K_{eq,4} = \frac{Y_{MEA} \cdot Y_{H_3O^+}}{Y_{MEA H^+}} \cdot \frac{C_{MEA} \cdot C_{H_3O^+}}{C_{MEA H^+}} = \exp\left(6.6942 - \frac{3090.83}{T_1}\right) \quad (28)$$

$$K_{eq,5} = \frac{Y_{MEA} \cdot Y_{HCO_3^-}}{Y_{MEA CO_3^-}} \cdot \frac{C_{MEA} \cdot C_{HCO_3^-}}{C_{MEA CO_3^-}} = \exp\left(-3.3636 - \frac{5851.11}{T_1}\right) \quad (29)$$

The overall material balances of MEA and CO₂ are as follow:

$$C_{0,MEA} = C_{MEA CO_3^-} + C_{MEA H^+} + C_{MEA} \quad (30)$$

$$\alpha_{CO_2} \cdot C_{0,MEA} = C_{MEA CO_3^-} + C_{HCO_3^-} + C_{CO_3^{2-}} + C_{CO_2} \quad (31)$$

The electroneutrality balance is as follow:

$$C_{MEA H^+} + C_{H_3O^+} = C_{MEA CO_3^-} + C_{HCO_3^-} + 2C_{CO_3^{2-}} + C_{OH^-} \quad (32)$$

$C_{0,MEA}$ is the total concentration (molarity) of MEA, α_{CO_2} is CO₂ loading. To perform chemical equilibrium calculation equations (25)-(32) (eight equations and eight variables) must be solved simultaneously to have the values of components concentration. The activity coefficients are calculated using the Wilson model.

2.5.2 Vapour-liquid equilibrium

In order to calculate the equilibrium partial pressure of CO₂, the empirical equations are utilized in this study. This method is reported in the literature [14]. Therefore, the experimental data [38] presented for 30, 45, and 60 wt% MEA solution that is in the concentration range of validation data are used to develop an empirical model to predict the equilibrium partial pressure of CO₂. Two different range of temperature is considered for the regression models. Therefore, the equilibrium partial pressure of CO₂ and the heat of desorption of CO₂ is calculated as follow:

$$P_{CO_2}^* = \exp\left(A + B\alpha_{CO_2} + CT \ln(\alpha_{CO_2}) + \frac{D}{T} + E \frac{\alpha_{CO_2}^2}{T^2} + F \frac{\alpha_{CO_2}}{T^2} + G \frac{\alpha_{CO_2}}{T}\right) \quad (33)$$

Table 1: The range of temperature and constants of equation (33) obtained by regression

	Temperature Range (°C)	A	B	C	D	E	F	G
30 wt%	40 < T < 80	38.98	58.8	0.006047	-12552	3712041	6363042	-42340
	80 < T < 120	34.30	-0.2	-0.00693	-16103	-380551	3704515	0
45 wt%	40 < T < 80	31	-52	0.006919	-9806	4046219	-7661695	36214
	80 < T < 120	54.29	-23.08	0.00873	-17790	3544895	1841414	0
60 wt%	40 < T < 80	42.24	-53	0.00728	-13546	4080073	-5113524	29182

80 < T < 120	137.2	-111.5	0.0618	-31177	12455987	510661	0
--------------	-------	--------	--------	--------	----------	--------	---

The coefficient of determination for all the regression models is higher than 0.90. Sakwattanapong et al. [39] discussed the importance of heat of absorption/desorption and reported that using constant values for heat of absorption/desorption will lead to inaccurate results. Therefore, using the regression model for the partial pressure of CO₂ and Gibbs-Helmholtz equation, the heat of desorption can also be calculated:

$$\frac{\Delta H_{Des}}{R} = \left[\frac{\partial \ln P_{CO_2}^*}{\partial \left(\frac{1}{T}\right)} \right]_P = C \frac{\ln(\alpha_{CO_2})}{T^2} - D - 2E \frac{\alpha_{CO_2}^2}{T} - 2F \frac{\alpha_{CO_2}}{T} - G\alpha_{CO_2} \quad (34)$$

Typical values of equilibrium partial pressure of CO₂ and heat of desorption calculated using equations (33) and (34) are illustrated in Table 2. As mentioned before the experimental data of equilibrium partial pressure of CO₂ are extracted from Aronu et al. [38]. It was tried to select the points that their CO₂ loadings are near to 0.4.

Table 2: Typical values of the equilibrium partial pressure of CO₂ and the heat of desorption of CO₂ (experimental data from Aronu et al. [38])

Concentration	T (°C)	α_{CO_2}	Pred. $P_{CO_2}^*$ (kPa)	Exp. $P_{CO_2}^*$ (kPa)	ΔH_{Des} (kJ/mol)
30 wt%	40	0.467	1.79	1.83	66.43
	60	0.428	2.50	2.79	85.15
	80	0.398	8.80	8.30	97.53
	100	0.409	44.70	42.19	69.20
	120	0.432	228.10	229.46	69.19
45 wt%	40	0.404	0.16	0.17	89.18
	60	0.392	1.20	1.42	82.37
	80	0.389	4.95	4.50	75.90
	100	0.445	96.83	96.88	114.23
	120	0.426	248.74	250.64	97.80
60 wt%	40	0.394	0.19	0.15	90.37
	60	0.424	3.24	3.03	81.35
	80	0.404	9.19	9.04	80.51
	100	0.386	30.64	30.94	167.72
	120	0.398	184.56	185.39	167.15

2.6 Methods for calculation of different parameters required for the modelling

The list of the methods and correlations that used in the current study to calculate the required physical properties and other parameters are illustrated in Table 3 and proper details about these correlations and methods can be found in Borhani et al. [23].

Table 3: Physical properties and other parameters used in the RPB stripper model

Property	Reference
Gas Viscosity	Multiflash package in gPROMS
Liquid Viscosity	[40]
Gas density	Multiflash package in gPROMS
Liquid density	[40] and [41]
Gas heat capacity	[10]
Liquid heat capacity	[42]
Gas side mass transfer	[43]
Liquid side mass transfer	[44]
Interfacial area	[43]
Henry's constant	[45]
Liquid diffusivity	Chilton and Colburn Analogy
Gas diffusivity	[46]
Thermal conductivity	Multiflash package in gPROMS
Pressure drop	[47]
Liquid holdup	[48]
Heat transfer coefficient	[49]
Vapor pressure	[10]
Activity coefficient	Wilson model [50]

As mentioned in Section 2.2, K-values are calculated using GA-MLR model and the regression constants are illustrated in Table 4. The genetic algorithm (GA) was used for the selection of the best parameters (feature selection) and functional form, by optimising with respect to the RQK fitness function [51], a constrained multi-criteria fitness function based on leave-one-out cross-validation variance (Q_{Loo}^2) and four simultaneous constraints [52]. This ensures that the final model is valid and has a good predictive capability, with limited correlation between the descriptors [52]. It should be noted that this correlation is applicable in a similar study on CO₂ capture using MEA. The general equation of K-values is as follow:

$$K - \text{value} = \exp(A + B x_{\text{CO}_2} + C x_{\text{H}_2\text{O}} + D x_{\text{MEA}} + E \ln T + F \ln P + G x_{\text{CO}_2} x_{\text{MEA}} + H \ln T x_{\text{CO}_2} x_{\text{H}_2\text{O}} + I x_{\text{MEA}} x_{\text{H}_2\text{O}} + J \ln P x_{\text{CO}_2} x_{\text{H}_2\text{O}}) \quad (35)$$

Table 4: Constants of equation (35) obtained by regression

	A	B	C	D	E	F	G	H	I	J
CO₂	144.19	-3.38	0	-16.3	-22.99	0.97	3.34	168.98	-1800.99	-24.33
H₂O	-32.1	34.3	-32.2	-32.9	10.878	-0.8658	0	0.412	0	
MEA	-161	45	41	38	19.728	-1.2434	0	0	2.56	

2.7 Implementation in gPROMS®

The gPROMS® Model Builder V4.2 is applied to implement the model. Similar to our previous study, the SRADAU solver based on Second-order Centred Finite Difference Method (CFDM) discretization method is used to solve the above-mentioned equations.

3 Model results and validation

The advantages of using MEA as solvent are its high CO₂ reactivity, high absorption capacity and low molecular weight and disadvantages of this solvent are the high heat of reaction and therefore high required energy for desorption [19]. Solvent concentration has an important effect on energy consumption in the stripper. It must be mentioned that the concentration of amine has a significant effect on desorption energy consumption in the stripper [5]. It is mean that by higher concentrations of amine the energy consumption could be reduced. In addition to RPB absorption experimental data presented by Jassim [27], the authors also performed experiments on desorption of CO₂ in the RPB stripper using MEA solution. In addition, Cheng et al. [5] presented desorption experimental data for 30 wt.% MEA solution. Therefore, these two sets of experimental data have been used in this study to validate the RPB stripper model. In addition, Cheng et al. [5] performed an experimental process analysis and investigated the impacts of rotational speed, liquid flow rate, reboiler temperature, and pressure on desorption efficiency and desorption energy. In Table 5, the specifications of RPB strippers from the two mentioned studies are presented. In addition, Table 6 shows the process conditions applied as inputs of the RPB stripper model. To have a better understanding of the model results, absolute relative deviation (ARD%) between experimental and predicted values of lean loading and reboiler duty is considered:

$$\text{ARD}\% = \left| \frac{X^{\text{Exp}} - X^{\text{Pre}}}{X^{\text{Exp}}} \right| \times 100 \quad (36)$$

where X is either lean loading or reboiler duty.

Table 5: Specifications of the RPB stripper

Parameter	[27]	[5]
Rotor speed (rpm)	600, 800, 1000	600, 900, 1200, 1500
RPB Diameter (m)	0.398 (OD), 0.156 (ID)	0.160 (OD), 0.076 (ID)
Packing Porosity (m ³ /m ³)	0.76	0.96
Packing type	Expanded stainless steel small mesh	Stainless wire mesh
Packing height (m)	0.025	0.020
Total surface area (a _t) (m ² /m ³)	2132	803

Table 6: Input to the RPB stripper model.

Jassim et al. [27]										
No	Rotor Speed	Flow rate		Pressure	Temperature (°C)		Rich MEA CO₂	Rich liquid wt. %		
	rpm	liquid (l/min)	steam (kmol/h)	atm	Reboiler	Rich amine	loading	H₂O	CO₂	MEA
1	800	36.8	11.1	1	94	68	0.4052	54.117	10.383	35.5
2	800	21.3	14.4	1	104	70	0.3456	61.536	7.664	30.8
3	600	30.2	13.9	1	118	58.9	0.4372	21.607	18.793	59.6
4	600	21.1	13.9	1	95.6	56.9	0.4305	26.491	17.409	56.1
5	1000	21.1	13.9	1	130.6	57.2	0.4217	25.142	17.458	57.4
6	1000	10.2	14.4	1	113	58.4	0.4028	32.895	15.105	52

Cheng et al. [5]											
No	Rotor Speed	Flow rate			Pressure	Temperature (°C)		Rich MEA CO₂	Reboiler duty (kW)		
	rpm	liquid (l/min)	steam (g/min)		atm	Reboiler	Rich amine	loading			
			CO₂	H₂O							
1	900	0.4	5.5	1.0	2	105	92.4	0.4840	0.62		
2	900	0.4	9.3	2.6	2	110	98.7	0.4840	0.80		
3	900	0.4	11.7	3.6	2	115	102.3	0.4840	0.90		
4	900	0.4	16.5	7.2	2	120	108.5	0.4840	1.24		
5	900	0.4	21.9	28.2	2	125	118.2	0.4840	2.01		

The reboiler heat duty has an inverse relation to the lean CO₂ loading, in which by increasing the lean CO₂ loading the heat duty will decrease [39]. This important point can be found in the experimental data presented by Cheng et al. [5] for example when the lean CO₂ loading is 0.4180 the reboiler duty is 0.62 kW and when the lean CO₂ loading is 0.2040 the reboiler duty is 2.01 kW.

Table 7: Comparison of experimental data with the results of the model

		Lean MEA CO ₂ loading			Heat duty of reboiler (kW)		
Jassim et al. [27]							
No	Rotor Speed (RPM)	Experimental	Prediction	ARD%	Experimental	Prediction	ARD%
1	800	0.3983	0.3924	1.4813	NA	-	-
2	800	0.3285	0.3159	3.8356	NA	-	-
3	600	0.4237	0.4093	3.3986	NA	-	-
4	600	0.4082	0.3845	5.8060	NA	-	-
5	1000	0.4027	0.4234	5.1403	NA	-	-
6	1000	0.3336	0.3153	5.4856	NA	-	-
Cheng et al. [5]							
No	Rotor Speed (RPM)	Experimental	Prediction	ARD%	Experimental	Prediction	ARD%
1	900	0.4180	0.4122	1.3876	0.6200	0.6394	3.1290
2	900	0.3700	0.3558	3.8378	0.8000	0.8120	1.5000
3	900	0.3400	0.3278	3.5882	0.9000	1.0089	12.1000
4	900	0.2710	0.2594	4.2804	1.2400	1.2820	3.3871
5	900	0.2040	0.1986	2.6471	2.0100	2.2100	9.9502

The experimental and predicted CO₂ loading in the lean MEA stream is compared in Table 7 for selected runs of two sets of experimental data. The comparison discloses that there is a good agreement between the experimental and predicted values. ARD% between the experimental and predicted CO₂ loading in lean MEA stream is in the range of 1.4813 to 5.8060 for data presented by Jassim et al. [27] and 1.3876 to 4.2804 for data presented by Cheng et al. [5]. As can be seen, the errors of the results are acceptable in engineering applications. Jassim et al. [27] did not present any data for heat duty of reboiler but Cheng et al. [5] presented these data. As can be seen in Table 6, the ARD% between the experimental and predicted heat duty of reboiler changed from 1.5 to 12. It must be mentioned that the result is in the range of study performed by Joel et al. (2017) as well.

4 Process analysis

In Section 3, it is shown that the model results have a proper agreement with the reported experimental data and hence the developed model can be used to investigate the behavior of the system by changing some variables. It should be noted that the validated model is utilized to perform the process analysis. By changing a parameter and fixing the other parameters the response of the model is examined. Two factors are utilized to examine the effect of changing variables. Desorption efficiency which characterises the amount of CO₂ existing in a stripped solution (ranges from 20 to 60% typically) can be calculated using the following relations [5]:

$$\text{Desorption efficiency} = \left(1 - \frac{\text{lean CO}_2 \text{ loading}}{\text{rich CO}_2 \text{ loading}}\right) \times 100 \quad (37)$$

The desorption energy which represents the amount of required energy to desorb one ton of CO₂ can be calculated using reboiler duty [5]:

$$\text{Desorption energy} = \frac{\text{Heat duty of reboiler}}{\text{mass of CO}_2 \text{ desorbed}} \quad (38)$$

As in RPB stripper in this study, we have a motor, the energy consumption by the motor should be accounted [53]:

$$P_{\text{motor}} = 1.2 + 0.1833 \times 10^{-7} \rho_1 R_o^2 \omega^2 Q_1 \quad (39)$$

where P_{motor} is motor power (kW), ρ_1 is the density of liquid phase (kg/m³), R_o is the outer radius of RPB (m), ω is angular velocity (rad/s), and Q_1 is the volumetric flow rate of lean MEA solution (l/min).

Therefore, another desorption energy by accounting motor power is considered in the study [26]:

$$\text{Desorption energy} = \frac{\text{Reboiler duty} + 2.5 \times P_{\text{motor}}}{\text{mass of CO}_2 \text{ desorbed}} \quad (40)$$

The motor power is multiplied by 2.5 which is thermal efficiency in conversion of thermal heat to the electricity. In this study, a comprehensive process analysis is considered. The effect of rotor speed, reboiler temperature, rich liquid flow rate, and pressure on desorption energy and desorption efficiency is examined. These parameters are selected based on the parameters investigated by Cheng et al. [5] in their experimental study. The RPB stripper utilized to perform the process analysis is same as characteristics described by Jassim et al. [27] in Table 5.

4.1 Effect of rotor speed

Rotor speed plays an important role in rotating packed bed system and hence this parameters should be analysed in modelling of RPB stripper. The effect of rotor speed on desorption efficiency and desorption energy are shown in Figure 1. The MEA concentration for this process analysis is 30 and 50 wt%, the reboiler temperature is 120 °C and the liquid flow rate is 18 l/min. As can be seen in 1000 RPM there is a maximum and after that, desorption efficiency is decreased. The rotor speed varied from 400 to 1200 rpm. It can be shown that the desorption efficiency is 32.9% at 400 rpm and 42.4 at 1200 rpm for 30 wt%. This parameter for 50 wt% changes from 20% at 400 rpm to 37.8% at 1200 rpm. Maximum desorption energy was observed at a rotor speed of 1000 rpm. It should be noted that the same trend and behaviour was reported by Cheng et al. [5] but the result is somehow different with the result of Joel et al. [26] for the effect of rotor speed on desorption efficiency. In this study, the desorption efficiency is reached to a maximum and then reduced but as is reported by Joel et al. [26] by increasing the rotor speed the desorption efficiency is increased. In the case of desorption energy, same trend and behaviour are illustrated in the work of Joel et al. [26]. The rotor speed and centrifugal force created small liquid droplets and consequently increase the mass and heat transfer area and hence the mass and heat transfer coefficients can be increased [23]. It must be mentioned that higher speeds can have a negative impact on the mass and heat transfer which is due to the reduction of the contact time between phases. Therefore, it is anticipated that there is an optimal rotor speed for the RPB stripper operation. The desorption energy is 7.1 GJ/ton CO₂ at 400 rpm and 4 GJ/ton CO₂ at 1200 rpm for 50 wt% solution. This parameter is 6.9 GJ/ton CO₂ at 400 rpm and 2.8 GJ/ton CO₂ at 1200 rpm for 30 wt%. It is interesting that for 50 wt% there is a minimum of desorption energy at about 1000 rpm but the desorption energy for 30 wt% is almost constant for a big range of rotor speed from 950 to 1200 rpm.

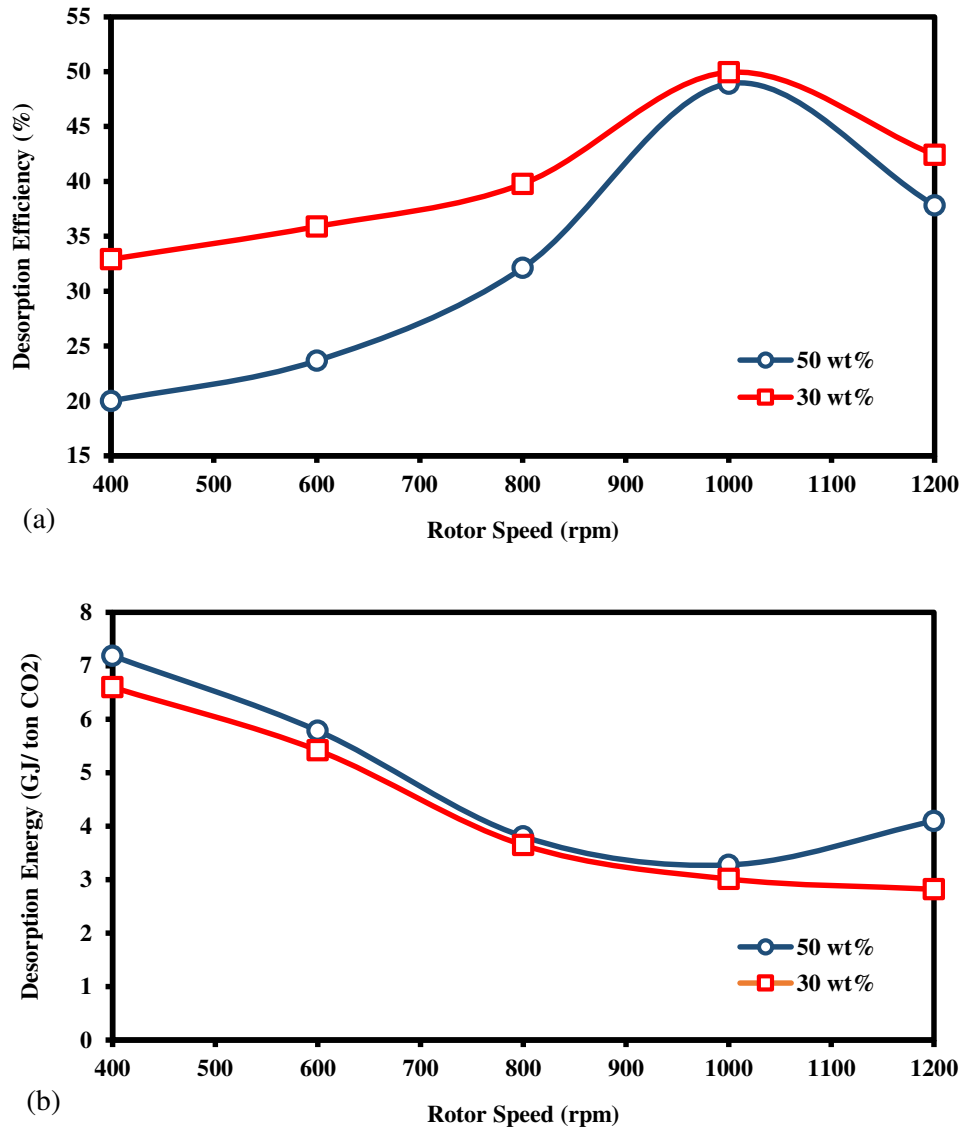


Figure 1: Effect of rotor speed on (a) desorption efficiency and (b) desorption energy of 30 and 50 wt% MEA solutions.

4.2 Effect of reboiler temperature

Another important and critical parameter for any type of stripper is the temperature of the reboiler. This parameter has an important effect on the energy consumption of the system. The effect of reboiler temperature on desorption efficiency and desorption energy for the 30 and 50 wt% MEA solutions is presented in Figure 2. The reboiler temperature is changed from 105 to 125 °C. More temperatures are avoided due to their bad effect on the solvent in the aspect of degradation. It can be seen from Figure 2 (a) that the desorption efficiency increased when increasing the reboiler temperature for both concentrations. The same behaviour is reported by Cheng et al. [5] and also Joel et al. [26].

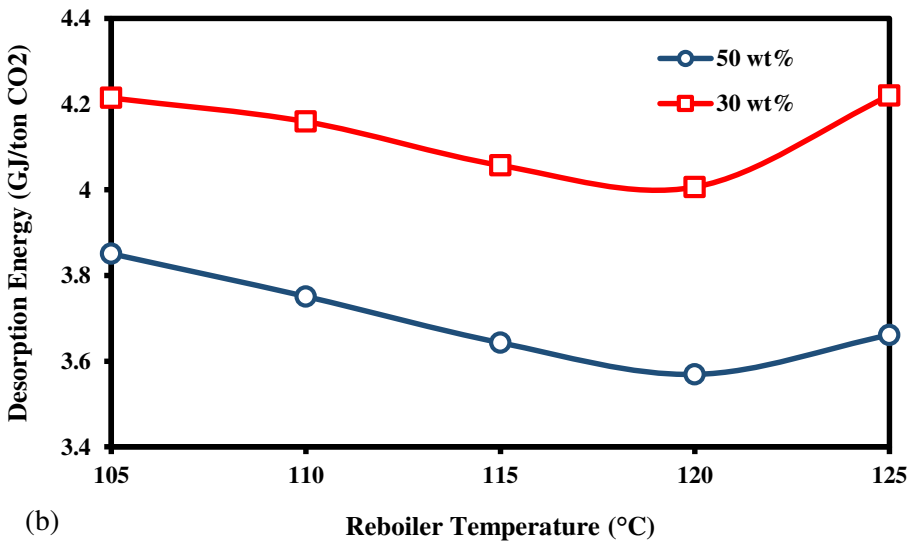
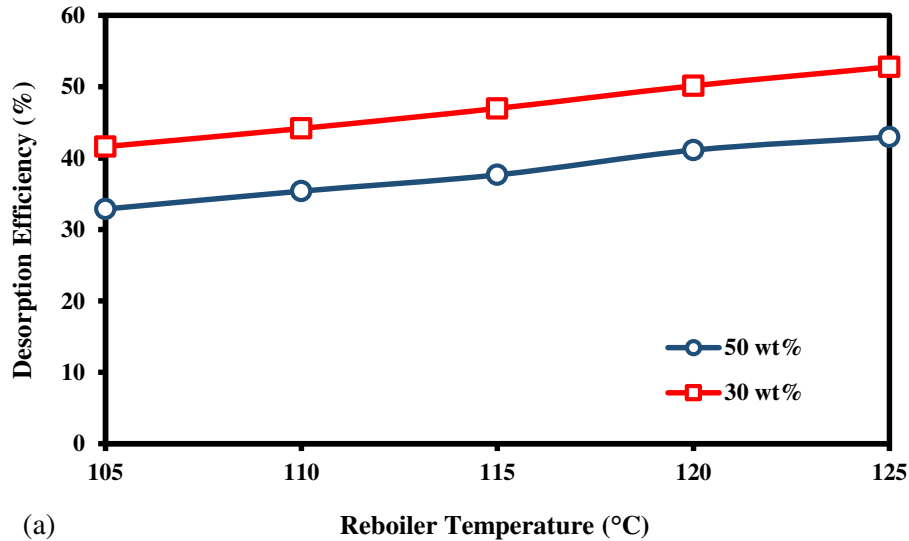


Figure 2: Effect of reboiler temperature on the (a) desorption efficiency and (b) desorption energy of 30 and 50 wt% MEA solutions.

On the other hand, the desorption energy decreased from 105 to 120 °C and then increased with further increases in the reboiler temperature. This trend also reported by Cheng et al. [5]. As the temperature was increased from 105 to 120 °C, the vapour pressures were increased and as a result, the rate of transfer of CO₂ and water from the liquid phase to the gas phase were increased. However, the vaporisation rate of water was higher than that of CO₂. Hence, a large amount of heat energy input will be consumed in the vaporisation of water. Therefore, the required energy for CO₂ desorption will start to increase as the reboiler temperature is raised beyond 120 °C.

4.3 Effect of rich liquid flow rate

The flow rate of the rich liquid is very important in analysing the strippers. This parameter is effective on the amount of stripped CO₂ from the stripper. It has also relevant to the reboiler duty. The effect of the rich liquid flow rate on the desorption efficiency and desorption energy is presented in Figure 3 for 30 and 50 wt%. The rich liquid flow rate altered from 10 to 30 l/min by 5 increments.

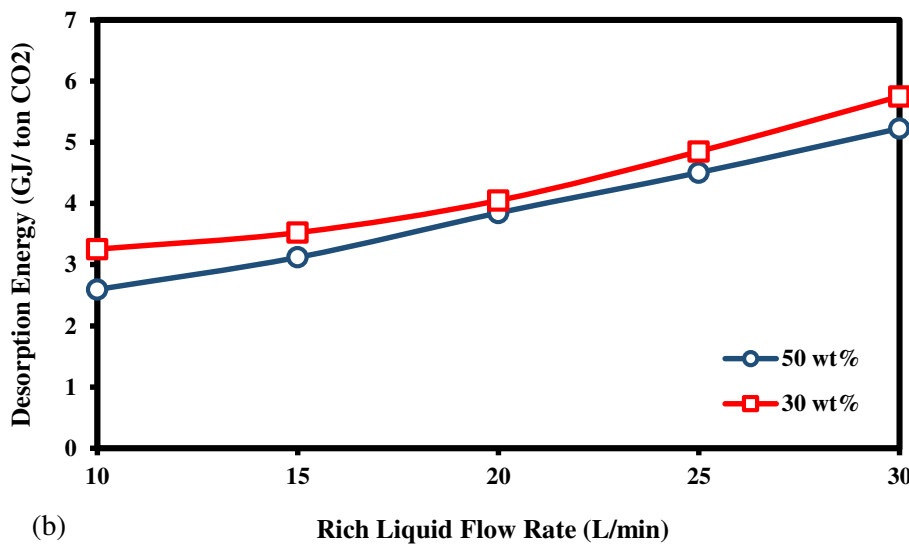
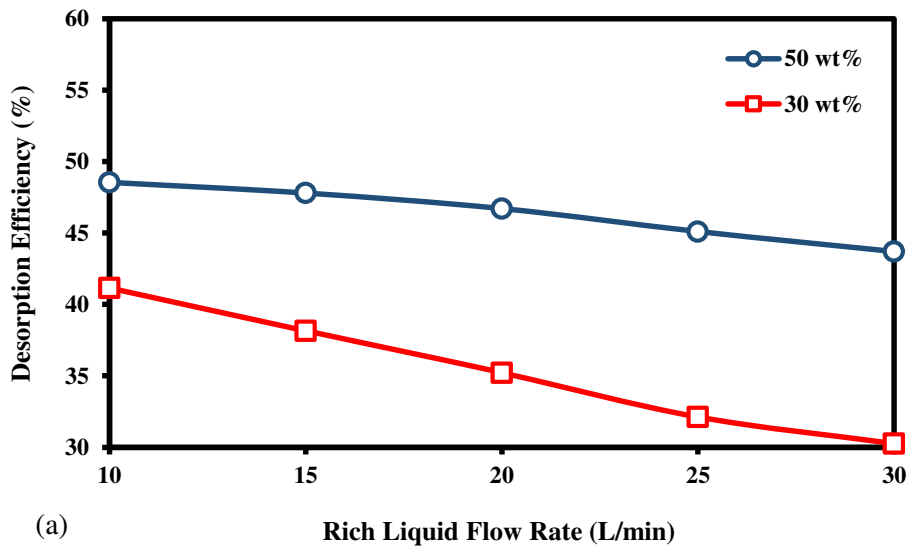


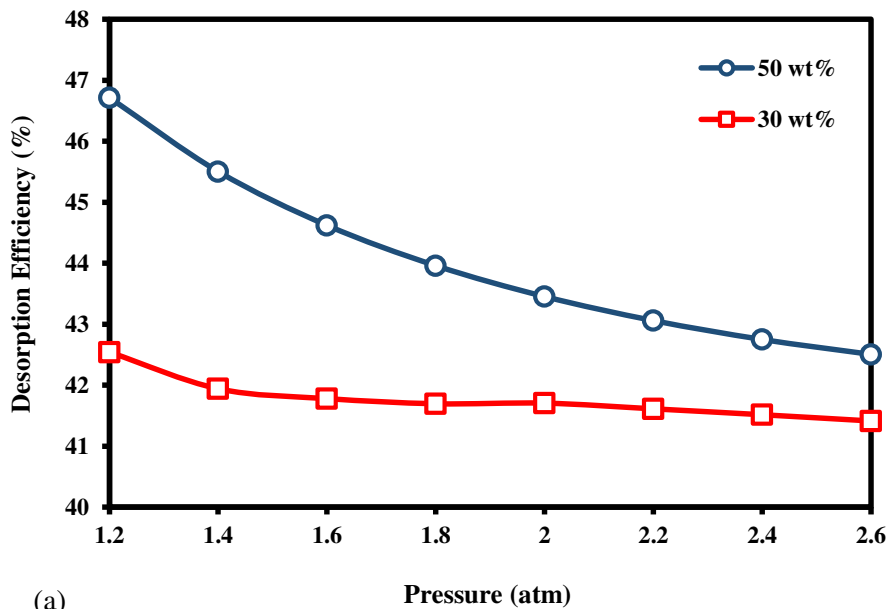
Figure 3: Effect of rich liquid flow rate on the (a) desorption efficiency and (b) desorption energy of 30 and 50 wt% MEA solutions.

By increasing the rich liquid flow rate from 10 to 30 l/min, desorption efficiency is decreased from 48.5% to 43.7% for 50 wt% and 41.1% to 30.2% for 30 wt%. Instead, desorption energy is increased

from 2.6 to 5.2 GJ/ ton CO₂ for 50 wt% and from 3.2 to 5.7 GJ/ ton CO₂ for 30 wt%. Although by increasing the liquid flow rate the mass and heat transfer coefficients and also the area of transfer will be increased but in another aspect, the contact time will be decreased by using higher liquid flow rates. This can justify why such behaviour is observed in Figure 3. In analysing this parameter by Joel et al. [26] they used a constant rich MEA loading and therefore, the desorption efficiency for all the cases became constant. The trend of showed diagram in Figure 3 is in complete agreement with the analysis of this parameter by Cheng et al. [5]. However, they reported the results for one concentration of MEA.

4.4 Effect of pressure

Different researchers reported the sensitivity of stripper to the pressure [18]. This operating parameter can play an important role in the stripper unit. The effect of pressure on the desorption efficiency and the desorption energy of 30 and 50 wt% MEA solutions are illustrated in Figure 4. The pressure is changed from 1.2 to 2 atm by using a liquid flow rate of 20 l/min at 120 °C. By increasing the pressure from 1.2 to 2 atm, desorption efficiency and desorption energy decreased monotonically. However, the decrease of desorption efficiency for 50 wt% is more than 30 wt% MEA solution.



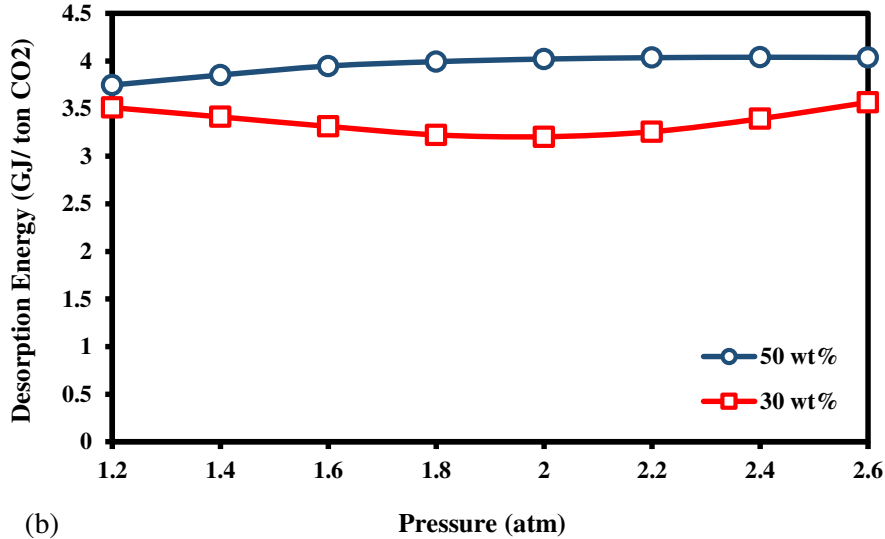


Figure 4: Effect of pressure on the (a) desorption efficiency and (b) desorption energy of 30 and 50 wt% MEA solutions.

There is a different trend for desorption energy which is related to the concentration of MEA. The result of desorption energy for 30 wt% confirms the discussion performed by Chen et al. [5]. They showed that for 30 wt% in the range of 2 to 2.5 atm the stripper works in good condition in the aspect of desorption efficiency and desorption energy. It must be mentioned that this process analysis was not reported by Joel et al. [26].

5 Conclusion

A detailed first principle distributed rate-based steady-state model for RPB stripper is developed and implemented in the gPROMS[®] model builder. Regression models are developed and utilized to calculate equilibrium partial pressure of CO₂, the heat of desorption of CO₂ and K-values. The developed model is validated using experimental data in the literature and showed good agreement. The concentration MEA solution in the study varied between 30-60 wt%. The ARD% between experimental and prediction values of CO₂ loading in lean MEA solution is in the range of 1.4813 to 5.8060 for data presented by Jassim et al. [27] and 1.3876 to 4.2804 for data presented by Cheng et al. [5]. The ARD% between the experimental and predicted heat duty of reboiler changed from 1.5 to 12 for data presented by Cheng et al. [5]. The AARD % for prediction of CO₂ loading in lean MEA stream presented by Jassim et al. [27] and Cheng et al. [5] is 4.19% and 3.14%, respectively. The AARD% for heat duty of

reboiler is 6.01%. Comprehensive process analysis performed on the validated model by considering different scenarios. Four parameters were varied to perform process analysis. The effect of rotor speed, reboiler temperature, rich liquid flow rate, and pressure on desorption energy and desorption efficiency is examined. The process analysis shows that by increasing the reboiler temperature desorption energy decrease to about 120 °C and after that this parameter increase. Modelling of the stripper system can provide insight into the desorption phenomena and result in optimal design.

Acknowledgement

The authors acknowledge financial support from the UK Engineering and Physical Sciences Research Council (EPSRC) (Ref: EP/M001458/2).

References

- [1] Z. Zhang, T.N.G. Borhani, M.H. El-Naas, in Chapter 4.5 - Carbon Capture A2 - Dincer, Ibrahim, C.O. Colpan, O. Kizilkan Eds., pp. 997-1016, Academic Press, (2018).
- [2] T.N.G. Borhani, A. Azarpour, V. Akbari, S.R. Wan Alwi, Z.A. Manan, International Journal of Greenhouse Gas Control, 41 (2015) 142-162.
- [3] F.A. Tobiesen, H.F. Svendsen, Industrial & Engineering Chemistry Research, 45 (2006) 2489-2496.
- [4] R.A. Frimpong, J.E. Remias, J.K. Neathery, K. Liu, International Journal of Greenhouse Gas Control, 9 (2012) 124-129.
- [5] H.-H. Cheng, C.-C. Lai, C.-S. Tan, International Journal of Greenhouse Gas Control, 16 (2013) 206-216.
- [6] M. Simioni, S.E. Kentish, G.W. Stevens, Journal of Membrane Science, 378 (2011) 18-27.
- [7] B.A. Oyenekan, G.T. Rochelle, AIChE Journal, 53 (2007) 3144-3154.
- [8] (!!! INVALID CITATION !!!).
- [9] B.A. Oyenekan, The University of Texas at Austin, (2007).
- [10] N. Harun, University of Waterloo (2012).
- [11] J. Oexmann, A. Kather, International Journal of Greenhouse Gas Control, 4 (2010) 36-43.
- [12] P. Galindo, A. Schäffer, K. Brechtel, S. Unterberger, G. Scheffknecht, Fuel, 101 (2012) 2-8.
- [13] X. Li, S. Wang, C. Chen, Energy Procedia, 37 (2013) 1836-1843.
- [14] B.A. Oyenekan, G.T. Rochelle, International Journal of Greenhouse Gas Control, 3 (2009) 121-132.
- [15] P. Mores, N. Scenna, S. Mussati, Energy, 45 (2012) 1042-1058.
- [16] R.H. Weiland, M. Rawal, R.G. Rice, AIChE Journal, 28 (1982) 963-973.
- [17] R. Khalilpour, A. Abbas, Separation and Purification Technology, 132 (2014) 149-167.
- [18] T. Li, T.C. Keener, International Journal of Greenhouse Gas Control, 51 (2016) 290-304.
- [19] F. Rezazadeh, W.F. Gale, Y.-J. Lin, G.T. Rochelle, Industrial & Engineering Chemistry Research, 55 (2016) 4622-4631.
- [20] M. Wang, A.S. Joel, C. Ramshaw, D. Eimer, N.M. Musa, Applied Energy, 158 (2015) 275-291.
- [21] K. Neumann, K. Gladyszewski, K. Groß, H. Qammar, D. Wenzel, A. Górak, M. Skiborowski, Chemical Engineering Research and Design, 134 (2018) 443-462.
- [22] S. Karmakar, A. Bhowal, P. Das, Chemical Engineering and Processing - Process Intensification, 132 (2018) 187-193.
- [23] T.N. Borhani, E. Oko, M. Wang, Journal of Cleaner Production, 204 (2018) 1124-1142.
- [24] E. Oko, C. Ramshaw, M. Wang, Applied Energy, 223 (2018) 302-316.

- [25] A.S. Joel, University of Hull, (2016).
- [26] A.S. Joel, M. Wang, C. Ramshaw, E. Oko, *Applied Energy*, 203 (2017) 11-25.
- [27] M.S. Jassim, G. Rochelle, D. Eimer, C. Ramshaw, *Industrial & Engineering Chemistry Research*, 46 (2007) 2823-2833.
- [28] C.C. Pantelides, M. Nauta, M. Matzopoulos, in *Equation-Oriented Process Modelling Technology: Recent Advances & Current Perspectives*, (2015).
- [29] J.M. Smith, H.C. Van Ness, M.M. Abbott, *Introduction to chemical engineering thermodynamics*, McGraw-Hill, (2005).
- [30] H.M. Kvamsdal, J.P. Jakobsen, K.A. Hoff, *Chemical Engineering and Processing: Process Intensification*, 48 (2009) 135-144.
- [31] N. Harun, T. Nittaya, P.L. Douglas, E. Croiset, L.A. Ricardez-Sandoval, *International Journal of Greenhouse Gas Control*, 10 (2012) 295-309.
- [32] D.M. Austgen, G.T. Rochelle, X. Peng, C.C. Chen, *Industrial & Engineering Chemistry Research*, 28 (1989) 1060-1073.
- [33] X. Luo, A. Hartono, S. Hussain, H. F. Svendsen, *Chemical Engineering Science*, 123 (2015) 57-69.
- [34] G. Astarita, D.W. Savage, *Chemical Engineering Science*, 35 (1980) 1755-1764.
- [35] F.A. Tobiesen, H.F. Svendsen, K.A. Hoff, *International Journal of Green Energy*, 2 (2005) 201-215.
- [36] T.J. Edwards, G. Maurer, J. Newman, J.M. Prausnitz, *AIChE Journal*, 24 (1978) 966-976.
- [37] R.L. Kent, B. Eisenberg, *Hydrocarbon Processing*, 55 (1976) 87-90.
- [38] U.E. Aronu, S. Gondal, E.T. Hessen, T. Haug-Warberg, A. Hartono, K.A. Hoff, H.F. Svendsen, *Chemical Engineering Science*, 66 (2011) 6393-6406.
- [39] R. Sakwattanapong, A. Aroonwilas, A. Veawab, *Industrial & Engineering Chemistry Research*, 44 (2005) 4465-4473.
- [40] R.H. Weiland, J.C. Dingman, D.B. Cronin, G.J. Browning, *Journal of Chemical & Engineering Data*, 43 (1998) 378-382.
- [41] C.-H. Hsu, M.-H. Li, *Journal of Chemical & Engineering Data*, 42 (1997) 502-507.
- [42] E.O. Agbonghae, K.J. Hughes, D.B. Ingham, L. Ma, M. Pourkashanian, *Industrial & Engineering Chemistry Research*, 53 (2014) 8291-8301.
- [43] K. Onda, H. Takeuchi, Y. Okumoto, *Journal of Chemical Engineering of Japan*, 1 (1968) 56-62.
- [44] H.-H. Tung, R.S.H. Mah, *Chemical Engineering Communications*, 39 (1985) 147-153.
- [45] J. Ying, D.A. Eimer, Y. Wenjuan, *Industrial & Engineering Chemistry Research*, 51 (2012) 6958-6966.
- [46] D.F. Fairbanks, C.R. Wilke, *Industrial & Engineering Chemistry*, 42 (1950) 471-475.
- [47] H. Llerena-Chavez, F. Larachi, *Chemical Engineering Science*, 64 (2009) 2113-2126.
- [48] J.R. Burns, J.N. Jamil, C. Ramshaw, *Chemical Engineering Science*, 55 (2000) 2401-2415.
- [49] T.H. Chilton, A.P. Colburn, *Industrial & engineering chemistry*, 26 (1934) 1183-1187.
- [50] J.M. Prausnitz, R.N. Lichtenthaler, E.G. de Azevedo, *Molecular Thermodynamics of Fluid-Phase Equilibria*, Pearson Education, (1998).
- [51] T.N.G. Borhani, M. Bagheri, Z.A. Manan, *Fluid Phase Equilibria*, 360 (2013) 423-434.
- [52] T.N.G. Borhani, M. Saniedanesh, M. Bagheri, J.S. Lim, *Water Research*, 98 (2016) 344-353.
- [53] S.P. Singh, J.H. Wilson, R.M. Counce, A.J. Lucero, G.D. Reed, R.A. Ashworth, M.G. Elliott, *Industrial & engineering chemistry research*, 31 (1992) 574-580.